# Supplementary Material

## Signature of the geometric phase in the wave packet dynamics on hypersurfaces

Hong-Guang Duan[1,2,3], Da-Long Qi[1,4], Zhen-Rong Sun[4], R. J. Dwayne Miller[1,3,5], and Michael Thorwart[2,3]
[1] *Max Planck Institute for the Structure and Dynamics of Matter, Luruper Chaussee 149, 22761 Hamburg, Germany*
[2] *I. Institut für Theoretische Physik, Universität Hamburg, Jungiusstraße 9, 20355 Hamburg, Germany*
[3] *The Hamburg Center for Ultrafast Imaging, Luruper Chaussee 149, 22761 Hamburg, Germany*
[4] *State Key Laboratory of Precision Spectroscopy, East China Normal University, 3663 North Zhongshan Road, 200062 Shanghai, China*
[5] *The Departments of Chemistry and Physics, University of Toronto, 80 St. George Street, Toronto Canada M5S 3H6*
(Dated: April 11, 2018)

This Supplementary Material provides the potential energy surfaces (PESs) for the parameter combinations involving a larger intersurface coupling between the two PESs. Moreover, we show the different projections of the wave-packet dynamics except from those on the $|\widetilde{e}_1\rangle$ PES which is depicted in Fig. 4 in the main text.

### I. POTENTIAL ENERGY SURFACE WITH $\Lambda = 400$, 600 AND 800 $\mathbf{CM}^{-1}$

Here, we show the PESs of the two configurations with a conical intersection (CI) and an avoided crossing (AC) of surfaces for different intersurface electronic coupling strength between two PESs. In Fig. S1, Fig. S2 and Fig. S3, we show the PESs for the electronic coupling between the two surfaces $\Lambda = 400$, 600 and 800 $\mathrm{cm}^{-1}$, respectively.

### II. WAVE-PACKET DYNAMICS FOR STRONG INTERSURFACE COUPLING

In this section, we show the dynamics of the wave packet for both the CI and the AC configuration in the regime of stronger intersurface coupling for $\Lambda = 400$, 600 and 800 $\mathrm{cm}^{-1}$. In particular, we show the kinetics of the wave packet on the upper electronic PES $|\widetilde{e}_2\rangle$ along the coupling mode $Q_c$ and the tuning mode $Q_t$ and of the wave packet on the lower excited PES $|\widetilde{e}_1\rangle$ along the tuning mode $Q_t$. The results for all values of $\Lambda$ are qualitatively similar and striking differences between the CI and the AC configurations occur only for the dynamics on the lower excited PES $|\widetilde{e}_1\rangle$ along the coupling mode $Q_c$, which we, thus, show in the main text.

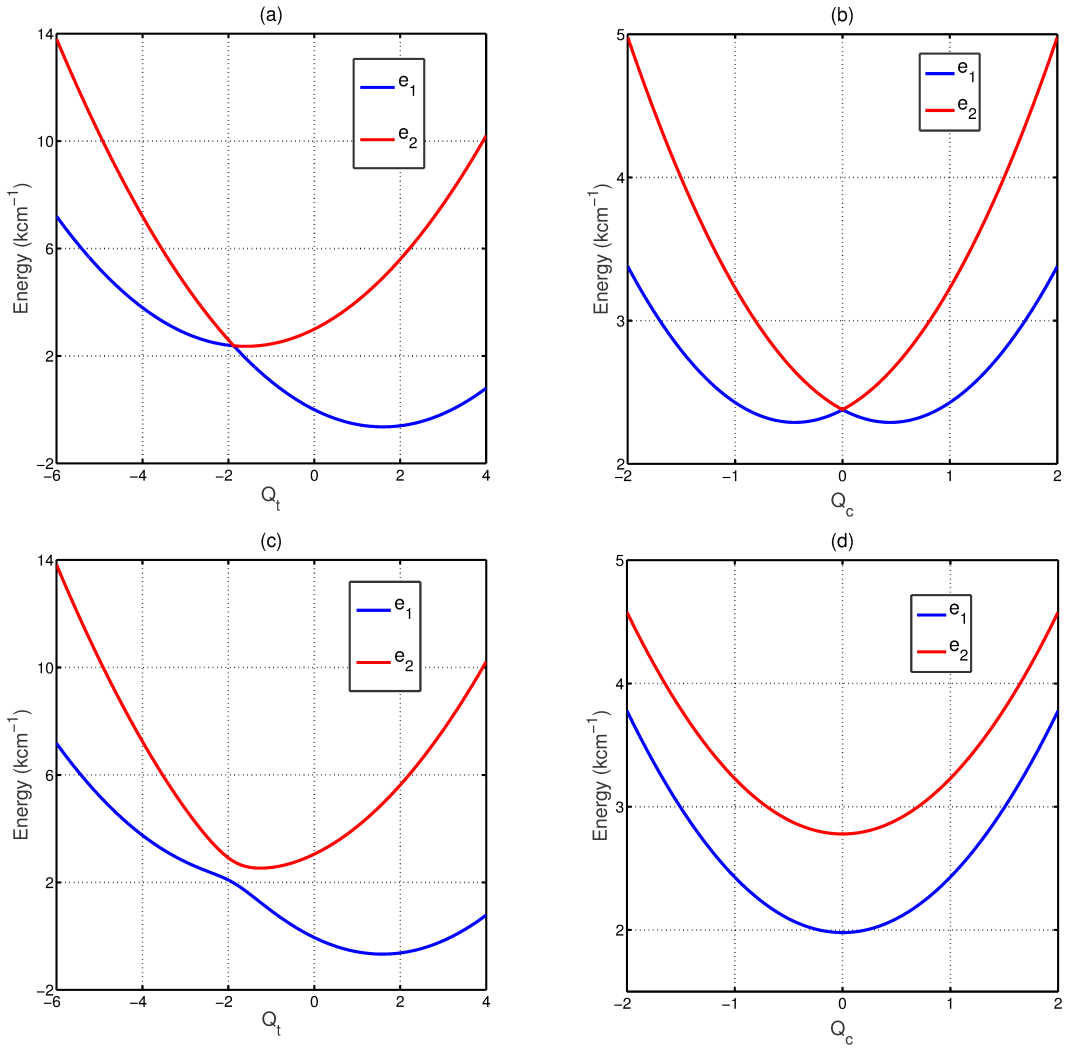


FIG. S1. PESs of the CI (a, b) and the AC (c, d) configuration along the tuning ($Q_t$) and the coupling ($Q_c$) modes for the intersurface coupling $\Lambda = 400$ cm$^{-1}$.

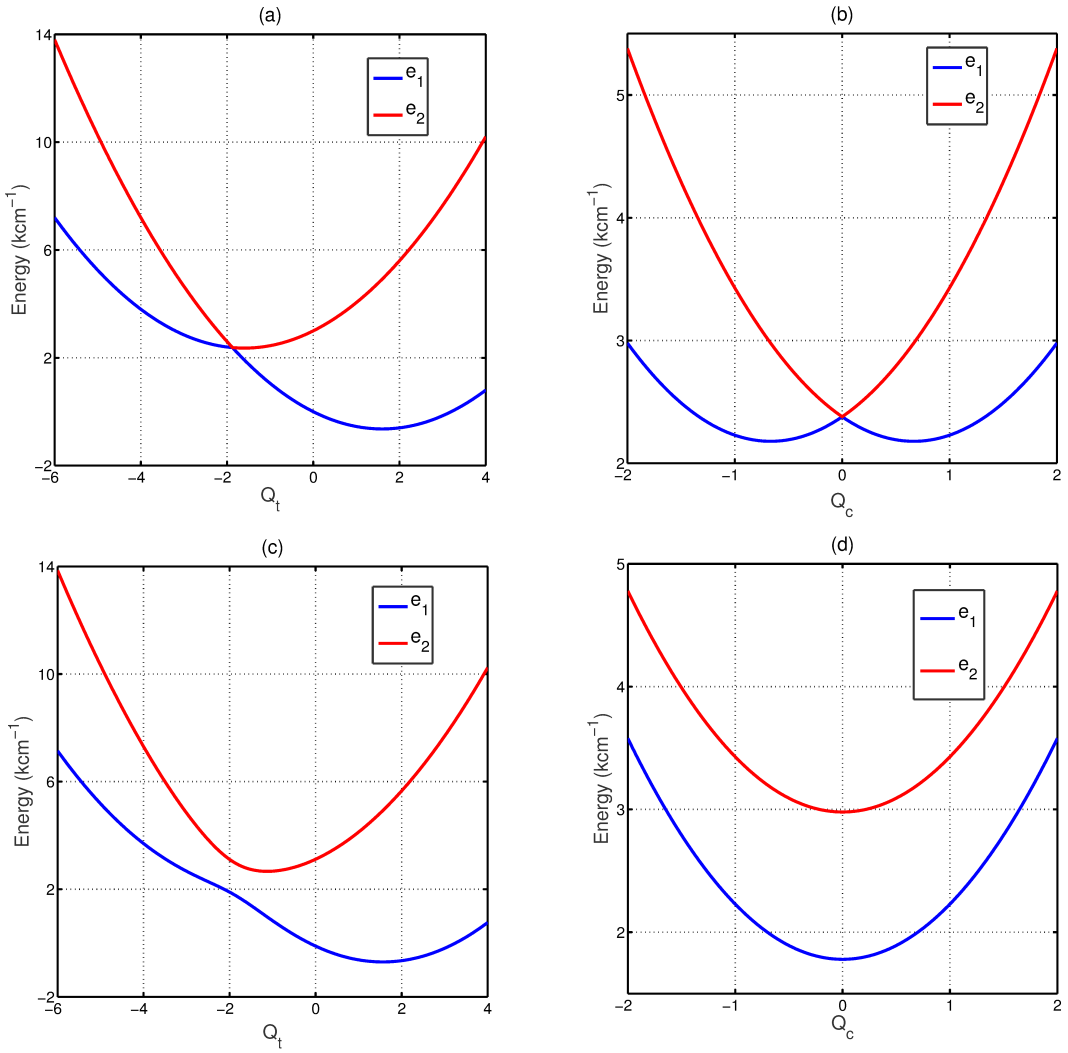


FIG. S2. Same as Fig. S1, but for $\Lambda = 600$ cm$^{-1}$.

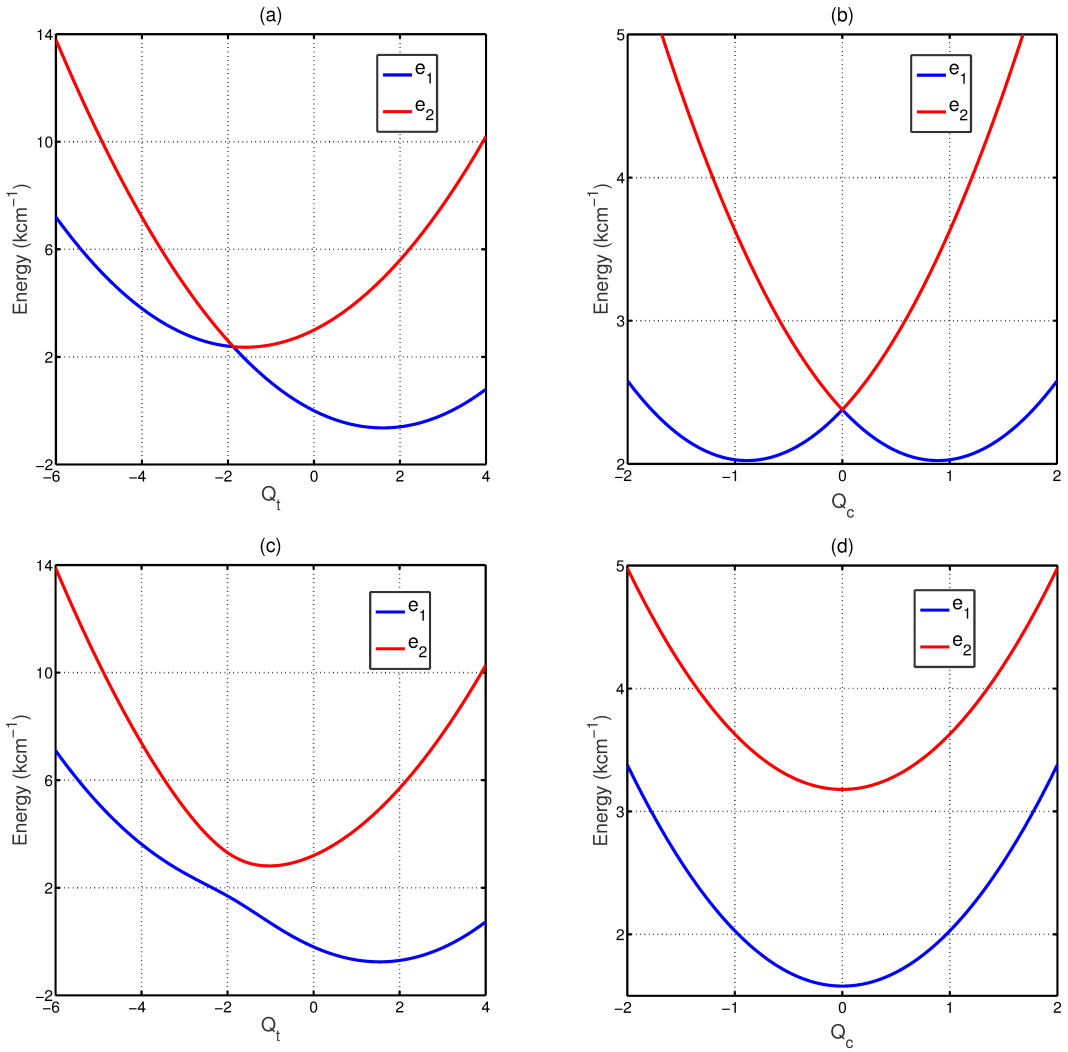


FIG. S3. Same as Fig. S1, but for $\Lambda = 800$ cm$^{-1}$.

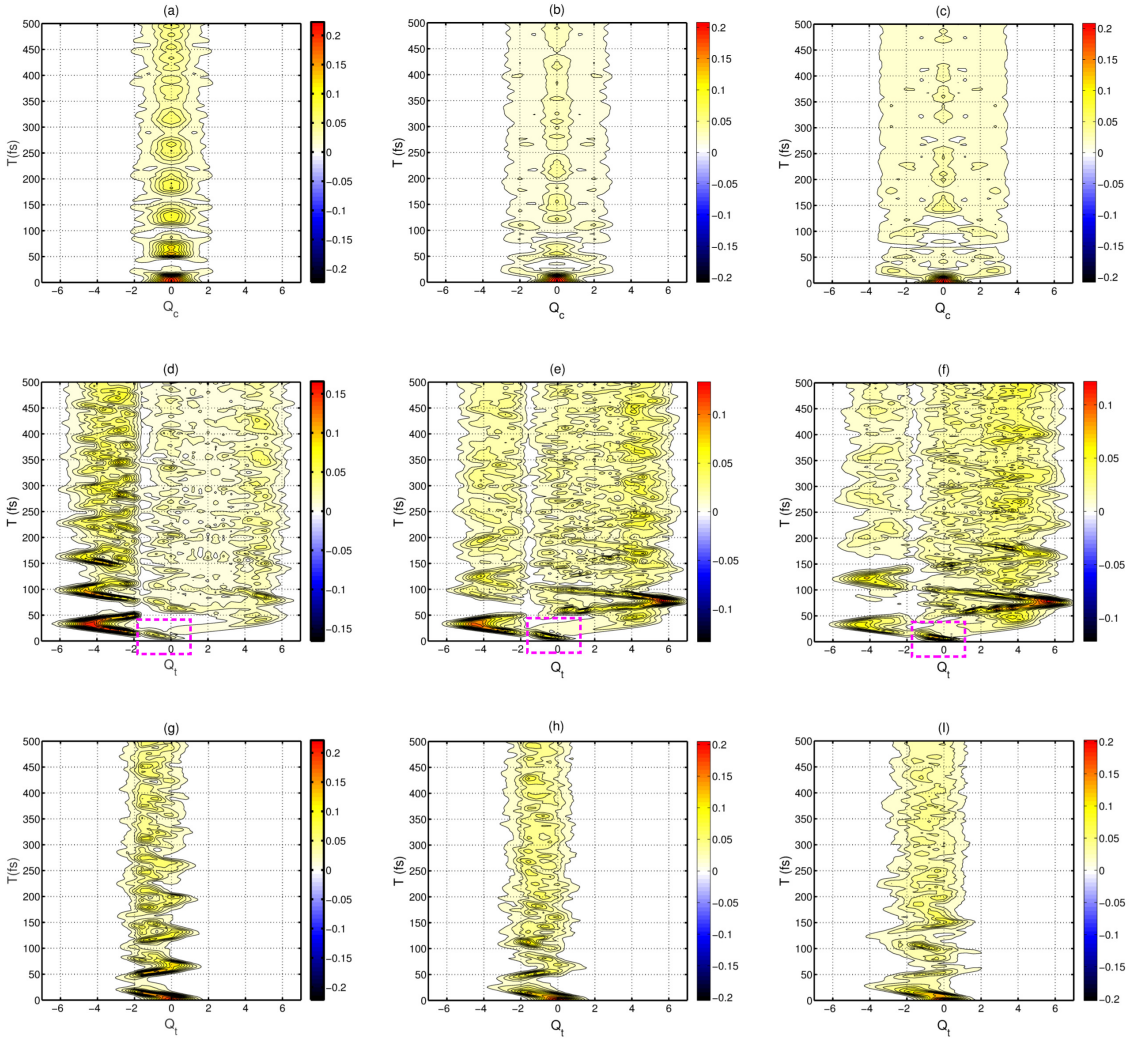


FIG. S4. The wave-packet dynamics of the CI configuration for $\Lambda = 400$ (a, d, g), 600 (b,e,h) and 800 (c, f, I) cm$^{-1}$. In (a), (b) and (c), the kinetics of the wave packet on the upper electronic PES $|\widetilde{e}_2\rangle$ is plotted along coupling mode $Q_c$. In (d), (e) and (f), we show the time evolution of the wave packet on the lower excited PES $|\widetilde{e}_1\rangle$ along the tuning mode $Q_t$. The wave-packet dynamics on the upper electronic PES $|\widetilde{e}_2\rangle$ is plotted along the tuning mode $Q_t$, respectively.

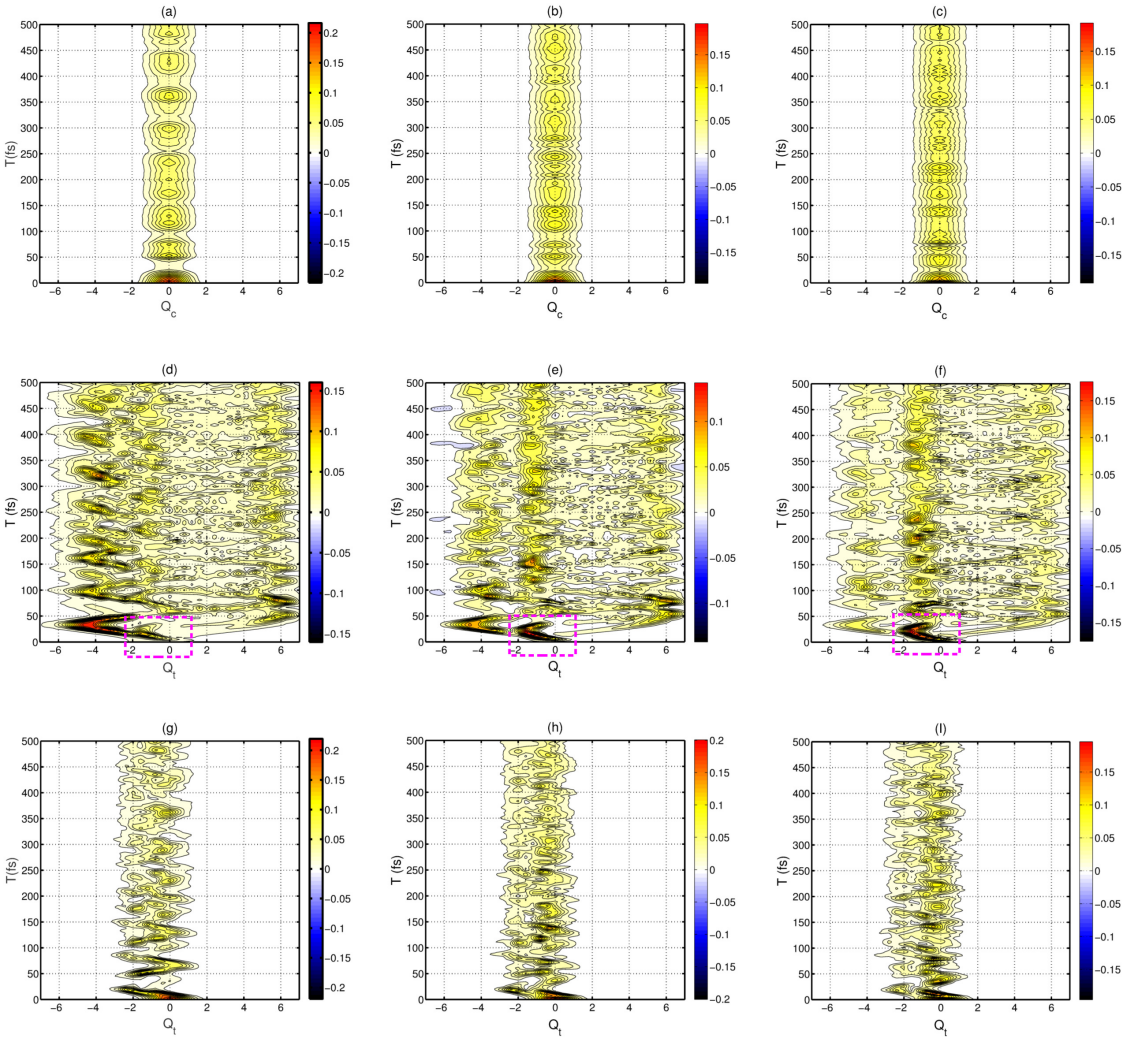


FIG. S5. Same as Fig. S4, but for the AC configuration.